Available on CMS information server **CMS CR 1998/005**

CMS Conference Report

February 20, 1998

Possibilities for $h^0 \to b\bar{b}$ with CMS at LHC

Lali Rurua

Institut für Hochenergiephysik, Österreichische Akademie d.Wissenschaften, Vienna, Austria

Institute of Physics of Georgian Academy of Sciences, Tbilisi, Georgia

For the CMS Collaboration

Abstract

We study the possibility of observing the lightest SUSY scalar Higgs h^0 in squark/gluino cascade decays exploiting its dominant decay mode $h^0 \to b\bar{b}$ with the CMS detector at the LHC. The study is done within the minimal Supergravity model. We find that there is a significant part of the mSUGRA parameter space where the $h^0 \to b\bar{b}$ peak can be observed with a signal to background ratio of ~ 1, and observation starts already at the low luminosity $L_{int} = 10^3$ pb^{-1}.

Presented at *5th International Conference on B-Physics at Hadron Machines*, Los Angeles, 13-17 October, 1997

1 Introduction

The main task of the LHC is to answer one of the fundamental questions of physics, namely: what is the origin of the particle masses? In the Standard Model (SM) particles acquire mass through their interaction with the Higgs field. The SM assumes one $SU(2)$ doublet of Higgs fields and has one physical Higgs boson (h^0_{SM}). Since there is a complete absence to date of any signals for new physics, the SM with a single neutral Higgs boson remains a viable model. However, there are simple extensions of the SM Higgs sector that are equally consistent with all known theoretical and phenomenological constraints. The Minimal Supersymmetric Standard Model (MSSM) contains two doublets of Higgs fields and five physical Higgs bosons ($h^0, H^0, A^0, H^{\pm}$).

In the supersymmetric scenario there is an upper bound on the mass of the lightest neutral Higgs boson (h^0). At tree-level this bound is (see e.g. Ref.[1]) $m_{h^0} \leq M_Z \mid \cos 2\beta \mid$, where $\tan\beta = v_u/v_d$ is the ratio of vacuum expectation values at M_Z. Radiative corrections can substantially raise the tree-level bound to $m_{h^0} \lesssim 130$ GeV [2]. The value of m_{h^0} mainly depends on m_A, $\tan\beta$, the stop and sbottom masses, and stop and sbottom mixings.

The theory does not predict the mass of h^0_{SM}, but it predicts its production rate and decay modes for a given mass, see [3]. CMS has been optimised for discovering the SM Higgs in the full expected mass range 0.08 TeV $\lesssim m_{h^0_{SM}} \lesssim 1$ TeV [4]. For $m_{h^0_{SM}} \lesssim 130$ GeV, the dominant decay channel $h^0_{SM} \to b\bar{b}$ [3] has very large Standard Model two-jet backgrounds. Thus, in this mass range, it is necessary to consider rarer production and decay modes with more pronounced characteristics. $h^0_{SM} \to \gamma\gamma$ was found to be the most promising channel for the low Higgs mass range, but high integrated luminosity is needed. The branching ratio Br($h^0_{SM} \to \gamma\gamma$) is $\sim 10^{-3}$ and the signal is expected on top of a large irreducible $\gamma\gamma$ background with a small S/B ratio of $\sim 1/20$ [5]. Moreover, instrumental requirements on ECAL are very demanding (a $\gamma\gamma$ effective mass resolution better than 1%, that is ≈ 1 GeV for a Higgs mass of 100 GeV). In the MSSM scenario $\sigma_{h^0} \times BR(h^0 \to \gamma\gamma)$ is even lower. A more advantageous way to look for h^0 can be found if one tries to use its abundant production in the decay chains of gluinos and squarks exploiting the dominant decay into $b\bar{b}$. In the MSSM, if gluinos and squarks are heavy enough they can decay into charginos and neutralinos. If, in turn, the mass difference between charginos and/or neutralinos is large enough, they can decay into a Higgs particle, see fig.1. The background can be suppressed by means of b-jet tagging and by requiring large E_T^{miss} characterising SUSY.

Here we discuss the possibility of observing a signal from the lightest neutral Higgs boson with the CMS detector at the LHC within the framework of the minimal Supergravity Model (mSUGRA) [6] with unification of the gauge couplings. The goal is to show the potential importance of b-flavour tagging for observing a signal from the lightest neutral Higgs boson at the LHC, which allows one to exploit its dominant decay mode, $h^0 \to b\bar{b}$. A more detailed analysis is presented in [7].

2 b-tagging performance

In this study we made use of the expected b-jet tagging performance of the CMS detector from impact parameter measurements in the tracker [8]. The CMS pixel detector consists of two cylindrically shaped barrel layers and three disk-like endcap layers (for more details, see [9]). The point resolution in barrel pixels is 15 μm. In the "high luminosity" configuration, optimised for b-tagging in hard collision physics up to the highest expected luminosities, the barrel layers are located at distances of 7.7 cm and 11.7 cm from the beam line and have a length of 36 cm, covering the rapidity range for tracks with $\mid \eta \mid \leq 1.75$. The three forward disks should provide at least two measurement points for tracks with $\mid \eta \mid < 2.4$. The "low luminosity" pixel detector option contains layers at r ≈ 4.0 and 7.7 cm and is optimised for b-tagging and B-physics measurements at the initial lower luminosities.

The expected precision of the impact parameter measurement in the CMS tracker has been studied by detailed GEANT simulations [10]. Fig.2 shows the impact parameter resolutions used in our simulations. The asymptotic value of the resolution is determined by the pixel point resolution and by the distance of the first measurement layer to the beam line.

To approximate the non-Gaussian tails in the impact parameter measurement distributions of the CMS detector the following procedure was applied. 2-jet events were generated with PYTHIA [11] at CDF energy $\sqrt{s} = 1.8$ TeV [8]. The distance of the first measurement layer from the beam line was taken at 3 cm, the same as the CDF tracker. Jets are reconstructed from the simulated data using the fast simulation package with the UA1 type jet finding algorithm. As for CDF data, the events are required to have at least one jet with $E_T^{jet} > 50$ GeV within $\mid \eta \mid < 2$. Only jets containing at least two tracks with $p_T > 2$ GeV are considered. The impact parameter is calculated for all tracks inside a jet ($\cos\Theta(jet - hadron) > 0.8$) with $p_T > 2$ GeV and smeared with its expected Gaussian error. The acceptance for hadron tracks is then limited to $\mid \eta \mid < 1.5$ corresponding to the fiducial volume of the

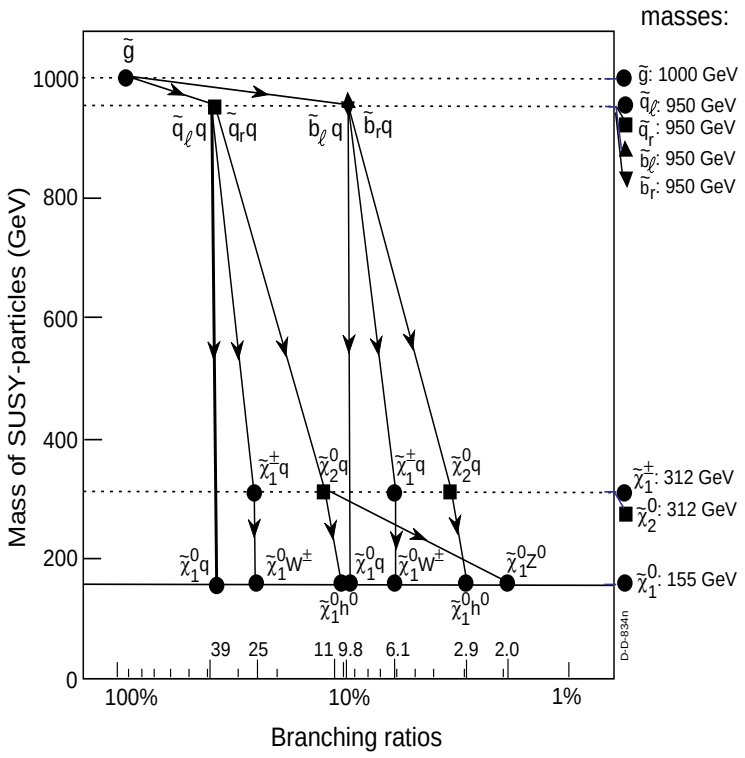

Figure 1: Gluino decay branching ratios in MSSM.

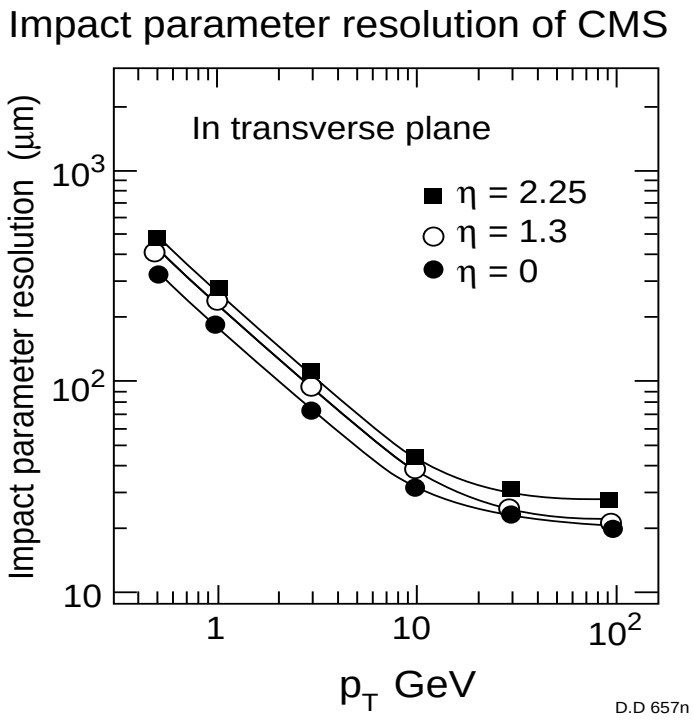

Figure 2: Impact parameter resolution as a function of p_t at various rapidities.

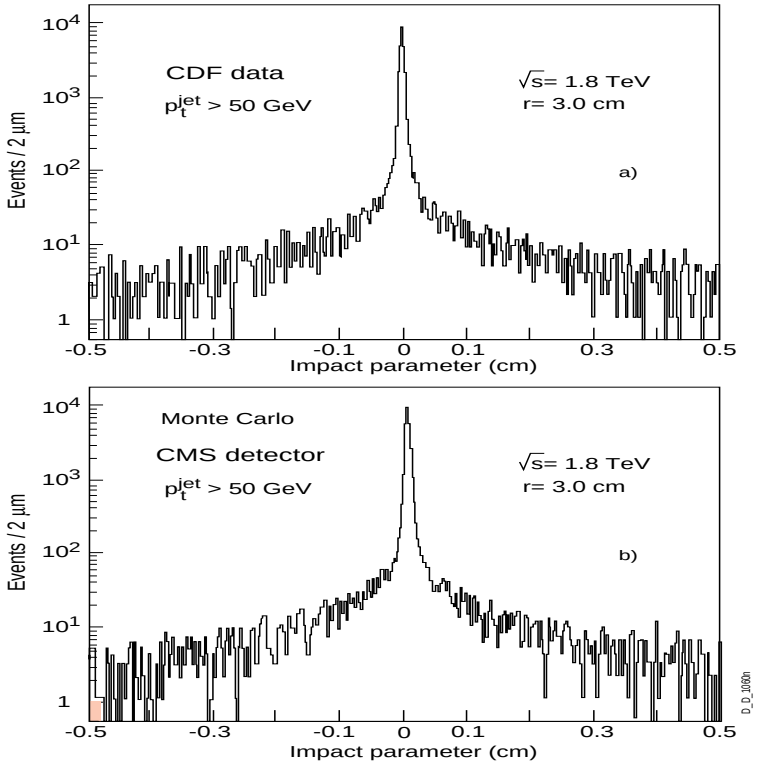

Figure 3: a) Impact parameter distribution measured by CDF collaboration, b) impact parameter distribution with CMS detector at $\sqrt{s} = 1.8$ TeV.

CDF microvertex detector. Fig.3b shows the impact parameter distribution calculated for the CMS detector with r=3 cm. The non-Gaussian tail present in this distribution is entirely due to heavy flavour and K_s^0 and Λ^0 decays. The relative level of the non-Gaussian tail in CDF data is about a factor 2 higher (fig.3a) than in the generated distribution (fig.3b). To simulate the impact parameter distribution for the CMS tracker at the LHC energies, we assume that the contribution to the tail due to "mismeasurements" (pattern recognition problems, noise, etc.) is the same measurement as at 1.8 TeV. Thus, the non-Gaussian tail in the CMS detector measurement simulation has been enhanced to match the relative fraction in the Gaussian part and in the tail as in the CDF data. Then the Gaussian part has been recalculated for the actual CMS pixel layers in terms of precision and radial distance, and for the kinematics corresponding to collisions at $\sqrt{s} = 14$ TeV. Fig.4 shows the expected b-tagging efficiency and mistagging rate in the CMS detector, which we have taken in our study as the 'nominal' b-tagging performance. The full pattern recognition studies of the CMS tracker response [12] done in the meantime match closely the results of the approximation used in the present study.

3 Signal observability in mSUGRA parameter space. Instrumental limiting factors

In mSUGRA the Higgs boson mass spectrum mainly depends on the following parameters: the universal scalar mass m_0, the gaugino mass $m_{1/2}$ at the GUT scale, and $\tan\beta$ [6]. It depends weakly on the other model parameters: A_0, the common trilinear coupling at M_{GUT}, and $sign(\mu)$, the sign of the Higgsino mixing parameter. Hence, we first discuss results in the $(m_0, m_{1/2})$ parameter plane fixing the other parameters, $\tan\beta$=2, $A_0 = 0$ and $sign(\mu) < 0$. Fig.5 shows the domain in the $(m_0, m_{1/2})$ parameter plane where the Higgs can be explored. This area is determined by the opening of the neutralino $\tilde{\chi}_2^0 \rightarrow \tilde{\chi}_1^0 h^0$ decays. The neutralinos $\tilde{\chi}_2^0$ can be produced in the gluino and squark decay chains. Thus, SUSY Higgs production is characterised by the presence of large E_T^{miss}, due to the weakly interacting lightest supersymmetric particle ($\tilde{\chi}_1^0$), high jet multiplicity from decays of gluinos/squarks and two b-jets from the $h^0 \rightarrow b\bar{b}$ decays. Additional b-jets can come from stop decays. Fig.6 shows the invariant mass distribution of two b-jets closest in $\eta - \phi$ space in the $ideal\ case\ of\ 100\%\ b-tagging\ efficiency\ and\ with\ 0\%\ mistagging\ probability$. The events are selected requiring at least 4 jets with $E_T^{jet} > 40$ GeV in $\mid \eta^{jet} \mid < 4.5$, at least 2 tagged jets in $\mid \eta^{jet} \mid < 1.75$, $E_T^{miss} > 400$

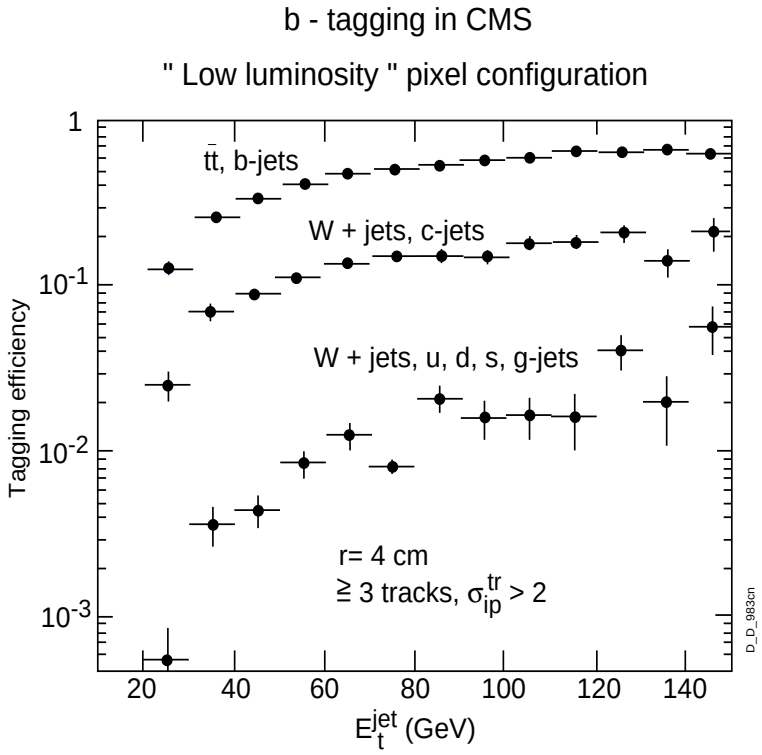

Figure 4: Expected b-tagging efficiency from the impact parameter measurement in the CMS tracker as a function of E_T^{jet}. At least three tracks ($p_T > 2$ GeV) with a transverse impact parameter of $> 2\sigma_{ip}$ are required in a jet.

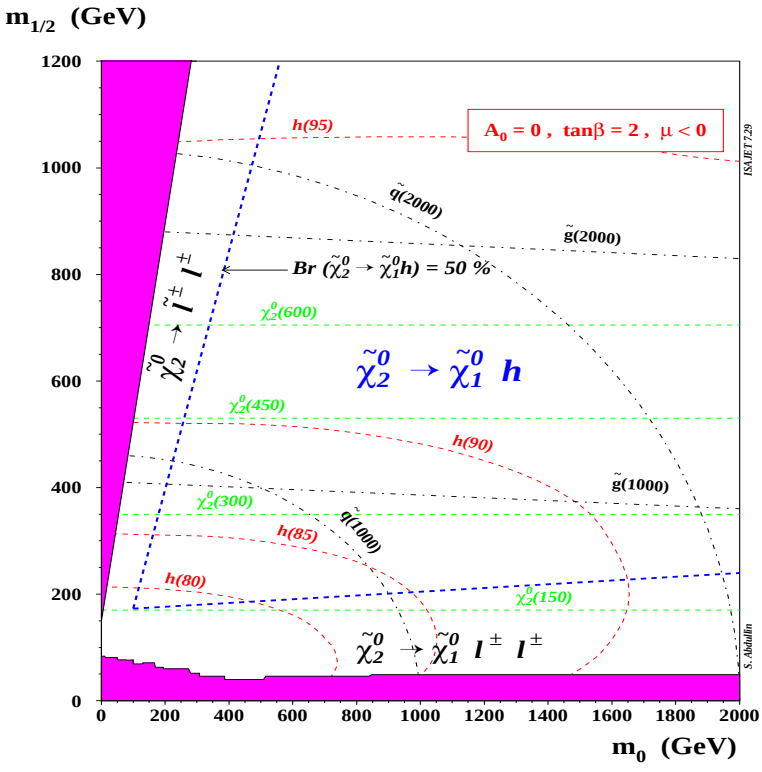

Figure 5: Domains of $\tilde{\chi}_2^0 \to \tilde{\chi}_1^0 h^0$, $\tilde{\chi}_2^0 \to \tilde{\chi}_1^0 l^+ l^-$ and $\tilde{\chi}_2^0 \to l^\pm \tilde{l}_{L,R}^\mp$ decays in the $(m_0, m_{1/2})$ parameter plane.

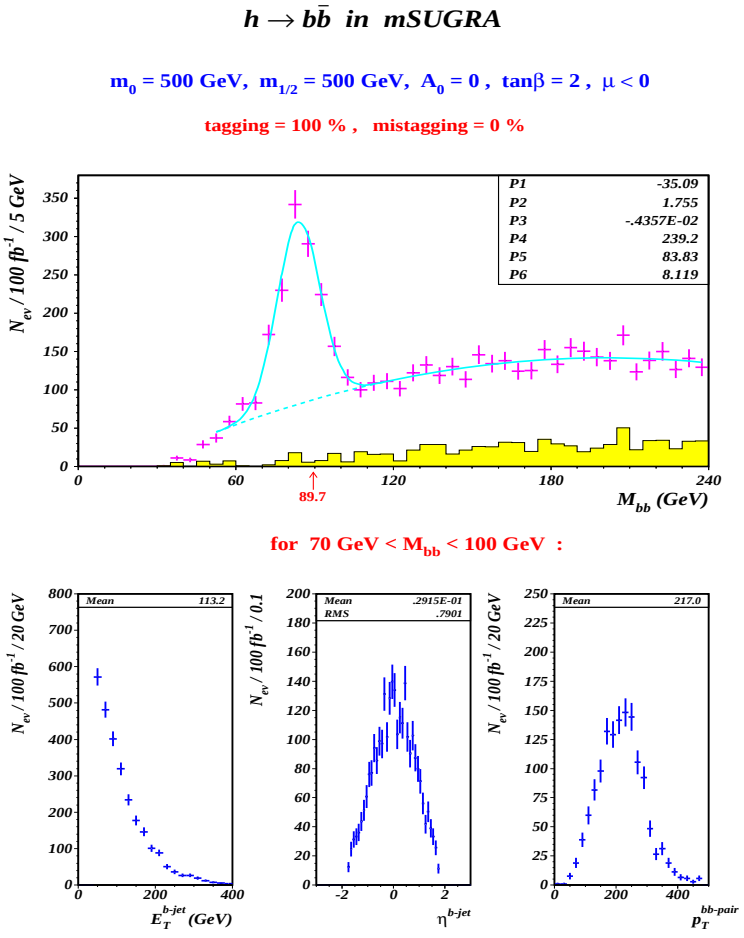

Figure 6: a) The invariant mass distribution of two b-jets at $m_0 = m_{1/2} = 500$ GeV, $\tan\beta = 2$, $\mu < 0$, $A_0 = 0$ mSUGRA point, assuming 100% tagging efficiency and 0% mistagging probability; b) b-jet energy distribution at the same parameter point, c) $\mid \eta \mid$-distribution of b-jets, d) p_T of bb-pair system.

GeV and $circularity > 0.1$. The E_T^{miss} cut is the most important background suppression cut. As a result the Higgs peak is clearly seen on top of the SM background ($t\bar{t}$, Wtb and QCD $2 \rightarrow 2$, including $b\bar{b}$). The main remaining background is internal SUSY background due to wrong b-jet pair combinations. Fig.6 also shows some kinematical distributions of b-jets. They are hard and central.

If we now include the nominal b-tagging efficiency and mistagging probability the Higgs peak is still well pronounced and the expected signal significance is $S/\sqrt{B} = 18.3$ for 10^5 pb^{-1}, see fig.7a. Figs.7b,c show the effect of increasing and decreasing the b-tagging efficiency by 15% in absolute value, keeping the mistagging probability on the 'nominal' level. The signal observability is very sensitive to the b-tagging efficiency, and degradation of that by more then 15% can result in a significant loss of the signal visibility, see fig.7c. Figs.8a,b show the dependence of signal visibility on the b-tagging acceptance. As shown above, b-jets are central. Thus an increase of b-tagging acceptance up to $\mid \eta^{tag} \mid < 2.4$ does not improve the signal significance, but keeping acceptance up to at least 1 is essential. Increasing the mistagging probability by a factor of 3 whilst keeping the 'nominal' b-tagging efficiency, decreases $S/\sqrt{B}$ down to 15.1. Another important criterion of the Higgs mass measurement is the width of the measured peak. The width of the measured di-jet invariant mass depends on the calorimetric jet measurement resolution. Fig.9 illustrates the degradation of the Higgs mass resolution due to degradation of the energy resolution in the hadron calorimeter from $\sigma_E/E = 82\%\sqrt{E} \oplus 6.5\%$ to $\sigma_E/E = 120\%\sqrt{E} \oplus 10\%$ (at $\eta = 0$). The signal width (σ Gaussian) changes from 7.6 GeV to 11 GeV.

By optimising the signal selection criteria in the various parts of the parameter space, we find large domains where the Higgs could be detected already at low luminosity, figs.10 and 11. The possibility of observing the

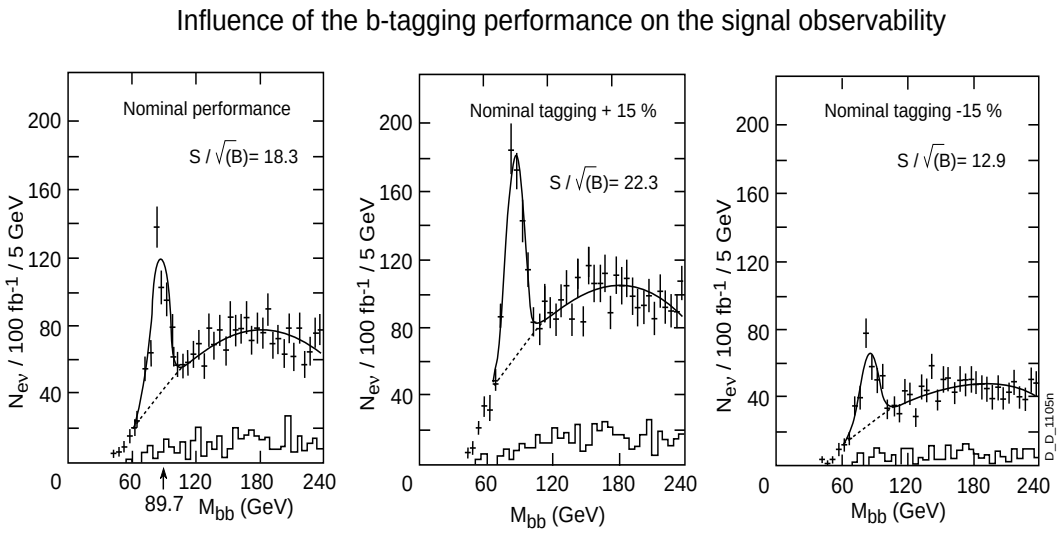

Figure 7: The invariant mass distributions of two b-jets at $m_0 = m_{1/2} = 500$ GeV, $\tan\beta = 2$, $\mu < 0$, $A_0 = 0$ mSUGRA point with a) 'nominal' b-tagging performance, b) b-tagging efficiency increased by 15% in absolute value and c) b-tagging efficiency decreased by 15%. Mistagging probability is on 'nominal' level in all cases.

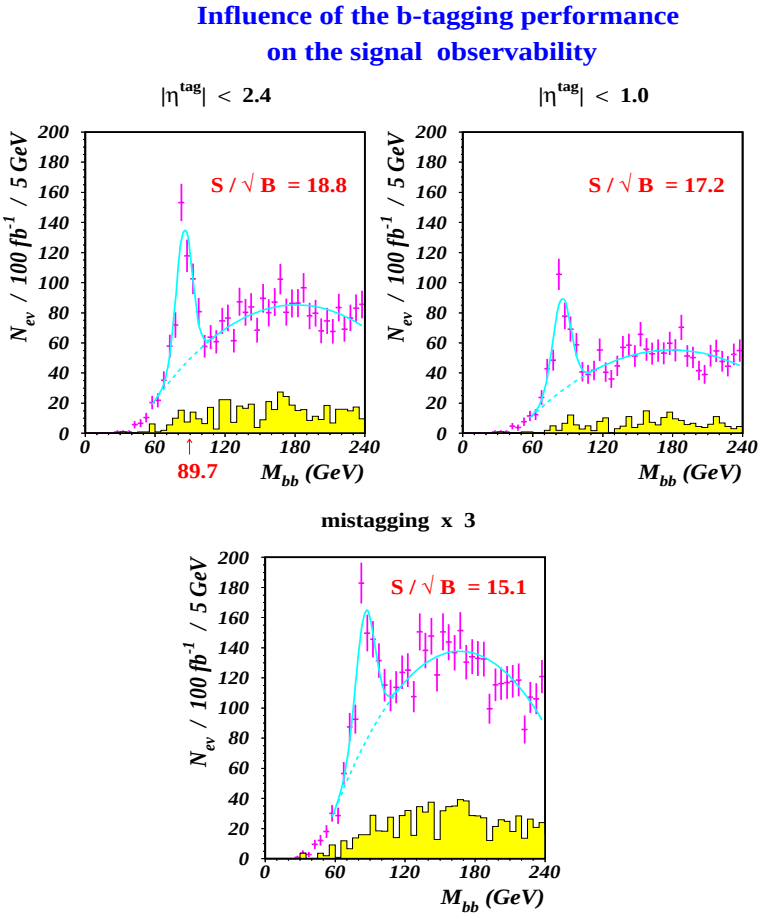

Figure 8: The invariant mass distributions of two b-jets at $m_0 = m_{1/2} = 500$ GeV, $\tan\beta = 2$, $\mu < 0$, $A_0 = 0$ mSUGRA point with a) tagging acceptance increased up to $\mid \eta^{tag} \mid = 2.4$, b) $\mid \eta^{tag} \mid = 1$ with 'nominal' tagging efficiency and mistagging probability; c) mistagging probability is increased by factor of 3.

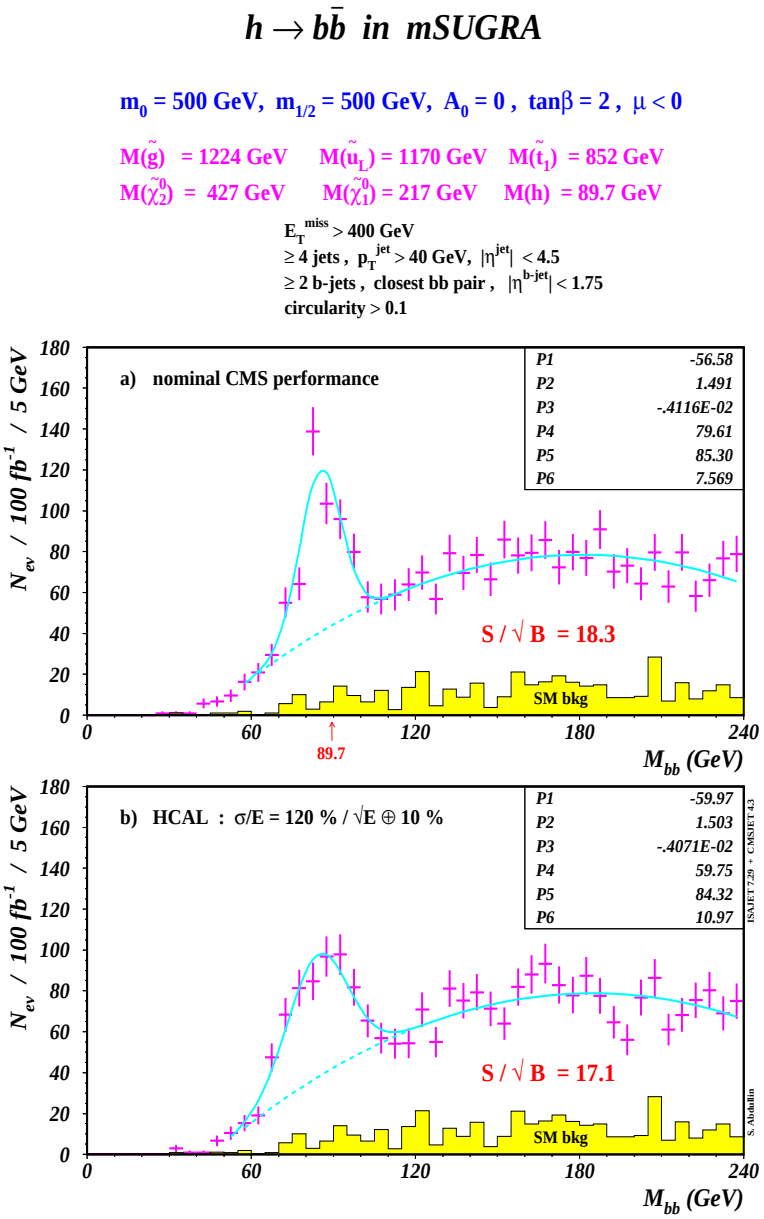

Figure 9: The invariant mass distributions of two b-jets at $m_0 = m_{1/2} = 500$ GeV, $\tan\beta = 2$, $\mu < 0$, $A_0 = 0$ mSUGRA point with a) energy resolution in hadron calorimeter $\sigma_E/E = 82\%\sqrt{E} \oplus 6.5\%$ and b) $\sigma_E/E = 120\%\sqrt{E} \oplus 10\%$ at $\eta = 0$.

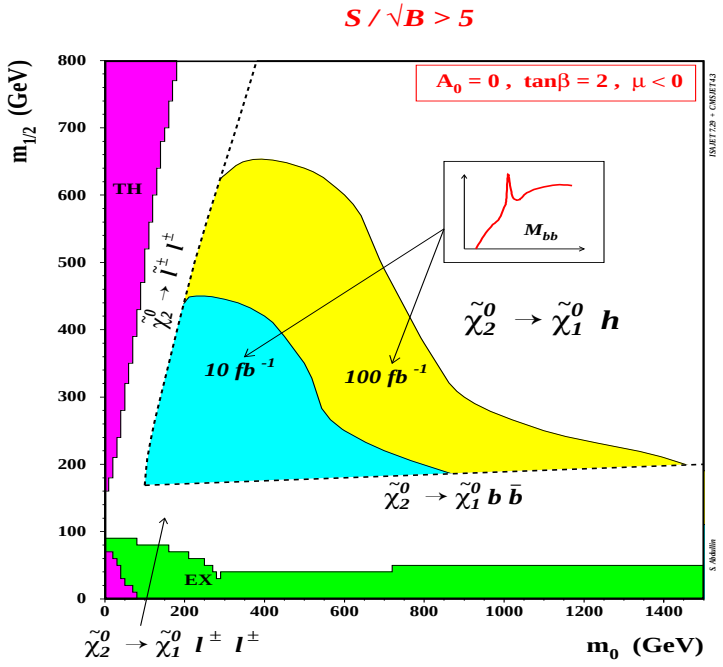

Figure 10: 5 σ contours of Higgs signal visibility in $(m_0, m_{1/2})$ mSUGRA parameter plane, $\tan\beta = 2$, $\mu < 0$, $A_0 = 0$.

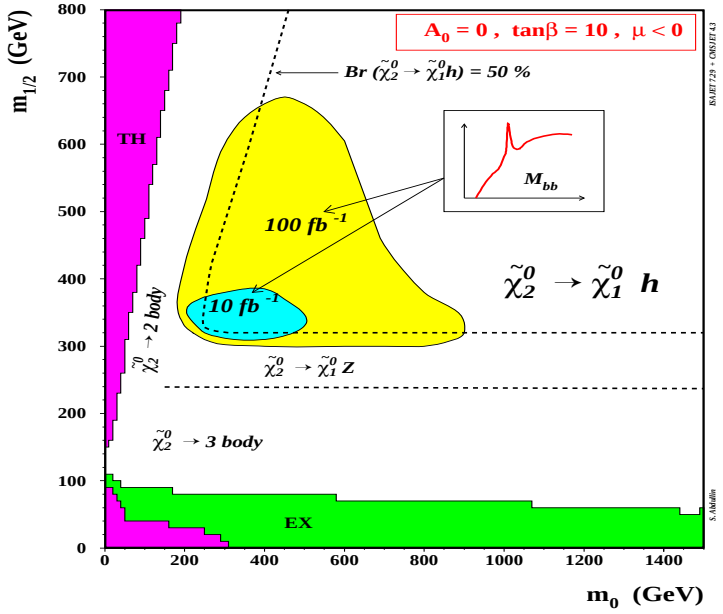

Figure 11: 5 σ contours of Higgs signal visibility in $(m_0, m_{1/2})$ mSUGRA parameter plane, $\tan\beta = 10$, $\mu < 0$, $A_0 = 0$.

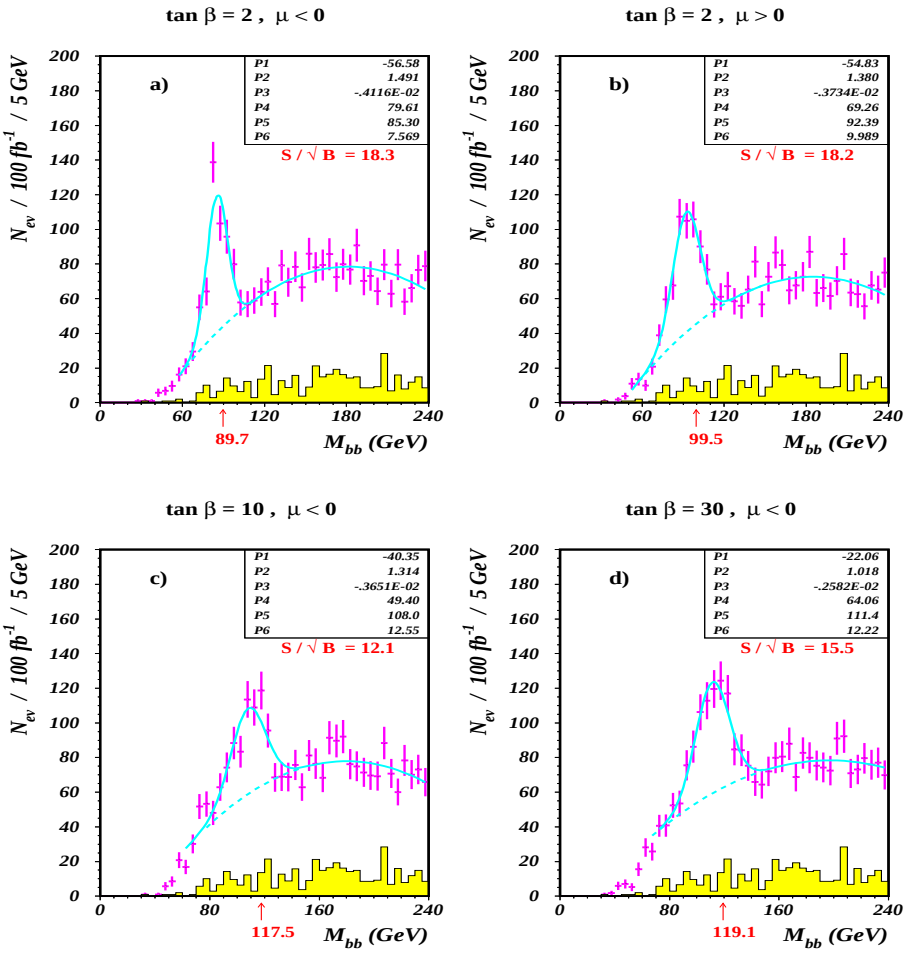

Figure 12: Dependence of Higgs signal visibility on mSUGRA parameters. Nominal b-jet tagging and detector performance.

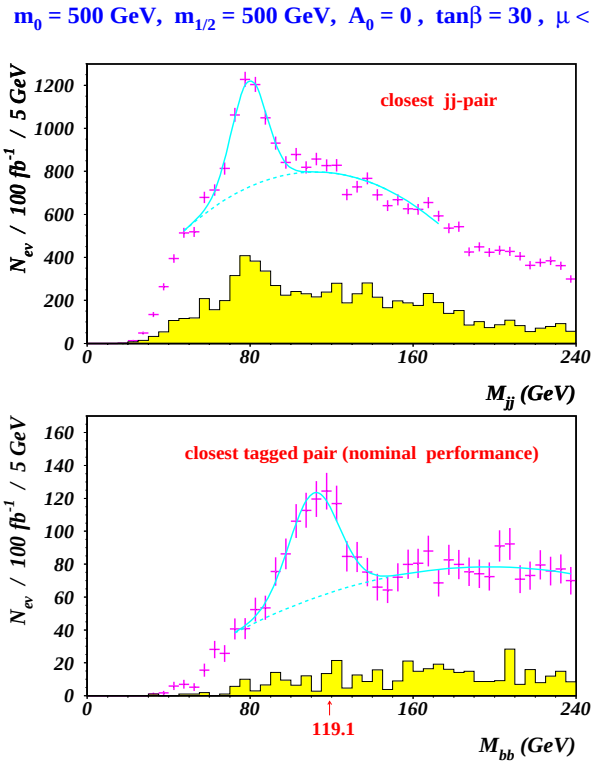

Figure 13: The invariant mass distributions for a) closest jet pairs and b) closest tagged b-jet pairs at $m_0 = m_{1/2} = 500$ GeV, $\tan\beta = 30$, $\mu < 0$, $A_0 = 0$ mSUGRA point with $m_{h^0} = 119.1$ GeV.

lightest SUSY Higgs is provided by the opening of $\tilde{\chi}_2^0 \to \tilde{\chi}_1^0 h^0$ decays and by the large production cross-section of strongly interacting gluinos and squarks. Its observation is therefore limited by the masses of the squarks and gluinos. In fig.12 we show the dependence of the signal visibility on the model parameters $\tan\beta$ and $sign(\mu)$ with fixed m_0 and $m_{1/2}$. The case $\tan\beta = 10$, $sign(\mu) < 0$ is the most unfavourable one due to less favourable values of Br($\tilde{\chi}_2^0 \to \tilde{\chi}_1^0 h^0$). The Higgs search strategy developed here shows that the large production cross-section of gluinos and squarks can allow one to exploit the dominant Higgs decay mode $h^0 \to b\bar{b}$ with background successfully suppressed by requiring large E_T^{miss}. Further, only efficient b-tagging allows one to reconstruct a real Higgs signal by suppressing the jet-jet SUSY background due to abundantly produced $W's$. Fig.13a shows the di-jet invariant mass for the closest jet pairs without b-tagging and where the $W-$peak overwhelms the Higgs signal. Fig.13b clearly exhibits that b-jet tagging is required to select the Higgs boson.

4 Conclusions

Adequate b-tagging performance is of crucial importance for the LHC experiments: it may allow one to discover $h^0(\to b\bar{b})$ with $S/B \sim 1$ in the whole h^0 mass range as shown here in the case of the mSUGRA model. Such a search can already start with $L_{int} = 10^3$ pb^{-1}.

Acknowledgements

I would like to thank Daniel Denegri and Walter Majerotto for their encouragement, fruitful discussions and help in the preparation of this contribution to the Conference. I thank also Michael Dittmar for interesting discussions.

References

[1] J.F. Gunion, H.E. Haber, G. Kane and S. Dawson, The Higgs Hunters Guide (Addison-Wesley Publishing Company, Redwood City, CA, 1990).

[2] H. Haber, T. Han, F.S. Merritt, J. Womersley, et al., hep-ph/9703391; J.F. Gunion, L. Poggioli, R. Van Kooten, C. Kao, P. Rowson et al., hep-ph /9703330, in Proceedings of the 1996 DPF/DPB Summer Study on New Directions for High Energy Physics, Snowmass, CO; H. Haber, Ringberg Workshop on the Higgs Puzzle, Ringberg Castle, Germany (1996), hep-ph/9703381;

M. Carena et al., hep-ph/9602250, in Vol. 1, Report of the Workshop on Physics at LEP2, G. Altarelli, T. Sjostrand and F. Zwirner (eds), CERN 96-01.

[3] A. Djouadi, J. Kalinowski and M. Spira, hep-ph/9704448.

[4] CMS Collaboration, Technical Proposal, LHCC/P2 (1994).

[5] R. Kinnunen, D. Denegri, CMS NOTE/1997-057.

[6] For reviews, see H.P. Nilles, Phys. Rep. **110**, 1 (1984);

P. Nath, R. Arnowitt and A. Chamseddine, Applied N=1 Supergravity, ICTP series in Theoretical Physics (World Scientific, Singapure, 1984);

M. Drees and S.P. Martin, hep-ph/9504324.

[7] S. Abdullin, D. Denegri, CMS NOTE/1997-070.

[8] R. Kinnunen, D. Denegri, CMS TN/96-045.

[9] Thomas Muller, these proceedings.

[10] V. Karimäki, Fast tracker Response Simulation, CMS-TN/94-275(1994).

[11] T. Sjöstrand, *Comp. Phys. Com.* **39**, 347 (1986);

T. Sjöstrand and M. Bengtsson, *Comp. Phys. Com.* **43**, 367 (1987);

H.U. Bengtsson and T. Sjöstrand, *Comp. Phys. Com.* **46**, 43 (1987);

T. Sjöstrand, CERN-TH.7112/93.

[12] A. Khanov, N. Stepanov, Presentation to the CMS Collaboration, November 1997.